R & D STATUS REPORT

CONTRACTOR: David Sarnoff Research Center

CONTRACT NO.: N00014-91-C-0216 **CONTRACT AMOUNT:** $1,585,150

EFFECTIVE DATE OF CONTRACT: 26 August 1991

EXPIRATION DATE OF CONTRACT: 25 August 1994

PRINCIPAL INVESTIGATOR: Dr. Edgar J. Denlinger

TECHNICAL CONTRIBUTORS: Dr. Aly Fathy, David Kalokitis,
Dr. Erwin Belohoubek,
Dr. K. S. Harshavardhan (Neocera),
Dr. Albert Piqué (Neocera),
Dr. T. Venkatesan (Neocera)

DARPA ORDER NO: 8100 **PROGRAM CODE NO:** DO-C9

TELEPHONE NO: (609) 734-2481

SHORT TITLE OF WORK: High Performance YBCO Films

REPORTING PERIOD: Period 5/1/92 to 7/31/92

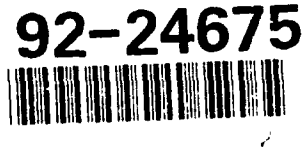

TABLE OF CONTENTS

DESCRIPTION OF PROGRESS:

SUMMARY

The objective of this program is to identify suitable low loss, low dielectric constant substrates and develop and optimize deposition processes for high quality YBCO films including the necessary buffer layers. Ultimate goals are large area substrates having double-sided HTS coating with a surface resistance ten times lower than copper at 40 GHz. High quality HTS films on low dielectric constant substrates are expected to find widespread use in advanced millimeter wave components, in extending the power handling capability of microwave and millimeter wave circuitry, and in facilitating high speed computer interconnects. Sample demonstration circuits will be built toward the end of the program.

The following progress report begins by describing our latest results with the development of both HTS film and substrate characterization methods in Section I. In cooperation with Cryo Industries we have completed the design of a three-axis positioning system for the dielectric resonator thin film test apparatus. This will allow us to efficiently probe a large wafer for surface resistance. A dielectrometer for measuring the dielectric constant of unmetallized substrates was received from Kent Laboratories and was used successfully at room temperatures. Calibrations at liquid nitrogen temperatures will be made soon. We continued investigating the cause of a low frequency roll-off in Q values for self-resonant HTS spirals. Various new ground plane configurations did not give us better results.

Because buffer layers are usually needed for successful deposition of YBCO on various dielectric substrates, we investigated their effect on microwave losses of microstrip lines with varying strip widths (or impedances). Our results show that moderate dielectric constants and loss tangents below 0.01 are desirable for

the buffer layer material. Also, the effect of the buffer layer becomes more and more significant for narrow lines, thin substrates, and at increasing frequency.

We started a theoretical investigation of the relative power handling capability of various resonator filter elements. A comparison between a microstrip line resonator and a disc resonator showed the latter to have significantly lower current densities and therefore higher power handling capability over a wide range of impedance levels.

Neocera has been working toward the goal of depositing high quality YBCO films on a low dielectric constant, low loss tangent substrate. During this period, effort has been concentrated on the use of strontium fluoride and quartz substrates. The best result with two buffer layers (MgO and YSZ) on SrF_2 was an onset temperature (Tc) of 82K and a transition width of < 2K. The major problem with quartz is a phase transformation occurring at 570 degrees C, which makes the material susceptible to thermal shock. With a YSZ buffer an onset temperature of 85K and a transition width of 5K was achieved. Recent success was demonstrated by Neocera (under a NASA Phase I program) on forming a free-standing YBCO film and attaching it to a diamond substrate. We are now exploring the possibility of extending this technique to a good low loss, low dielectric constant substrate under this contract.

I. SUPERCONDUCTOR SAMPLE CHARACTERIZATION AT MICROWAVE FREQUENCIES

A. HTSC Film Characterization

We have worked closely with Cryo Industries (Atkinson N.H.) to design a 3 axis positioning system for the dielectric resonator thin film test system. The system will allow scanning of wafers up to 5 cm diameter while performing microwave surface resistance measurements over a 15-300K temperature range.

Long travel micrometers will allow accurate positioning to 1 mil. The key requirements for the system will be to repeatably position the sample accurately with a low thermal load and good sample temperature control. This is acheived by using a low thermal conductance arm to position the sample and copper braid straps between the sample holder and the cold finger. A sketch of the system is shown below in Fig. 1. A z-axis drive is included to raise and lower the sample to avoid scratching the HTS film when moving the sample in the x-y planes. We have received a quote to construct this hardware for $7K from Cryo Industries. This system will be constructed and tested during the next report period.

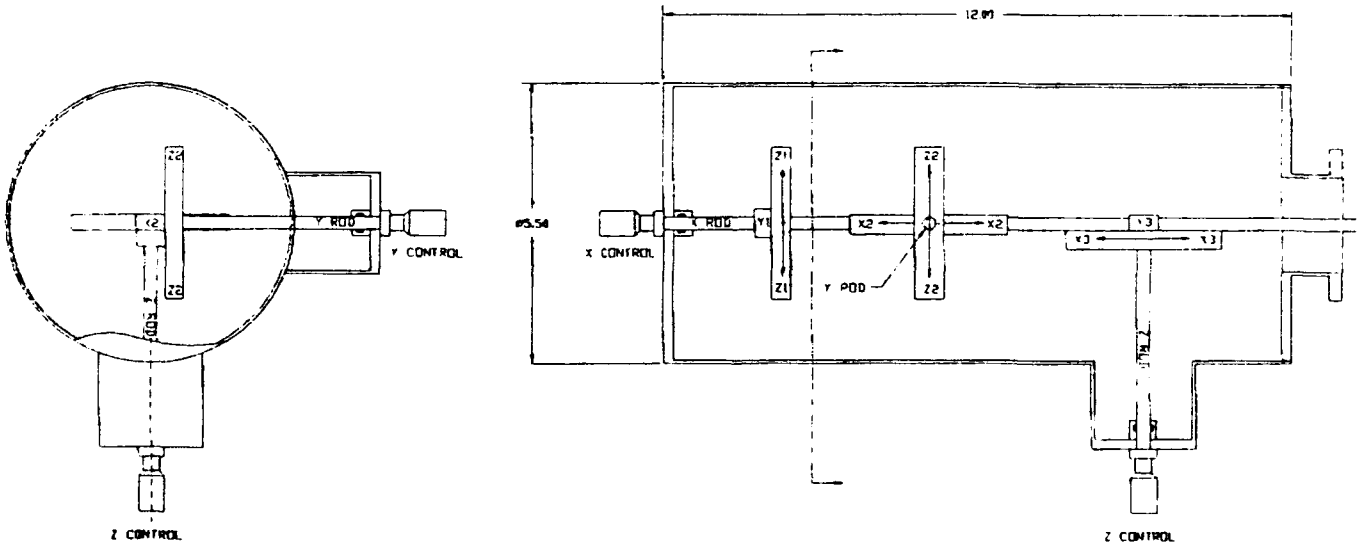

Fig. 1. Three axis positioning system.

B. Substrate Characterization

A dielectrometer was received from GDK Products for the measurement of unmetallized substrate dielectric constant and loss tangent at microwave frequencies. The instrument was checked out and calibrated; room temperature measurements were made on various substrates of interest. One set of measurements on cordierite ceramic material obtained from GEC Marconi and Trans Tech resulted in dielectric constants around 5 and loss tangents around 0.0001. Thermal expansion coefficients supplied from the vendors varied between 3 and 5 x 10-6 per degree C, which is a factor of 2 - 3 less than that of the YBCO film. This substrate may be a good candidate for use with a free-standing YBCO film. The dielectrometer must be calibrated at 77K before evaluating substrates at cryogenic temperatures.

II. SELF-RESONANT SPIRALS FOR HTS SAMPLE CHARACTERIZATION AT VHF/UHF FREQUENCIES

We continued investigation of a low frequency roll off in Q values for the self-resonant spirals reported in the last quarterly report. The possibility of losses due to the lack of a suitable ground connection between the HTS ground plane and the test fixture in the microstrip configuration was addressed. Fig. 2 depicts two copper ground straps attached to the ground plane substrate using silver loaded paint. The structure was measured and there was no change observed after the addition of the straps. The data is plotted in Fig. 3 and labeled Microstrip, HTS ground plane.

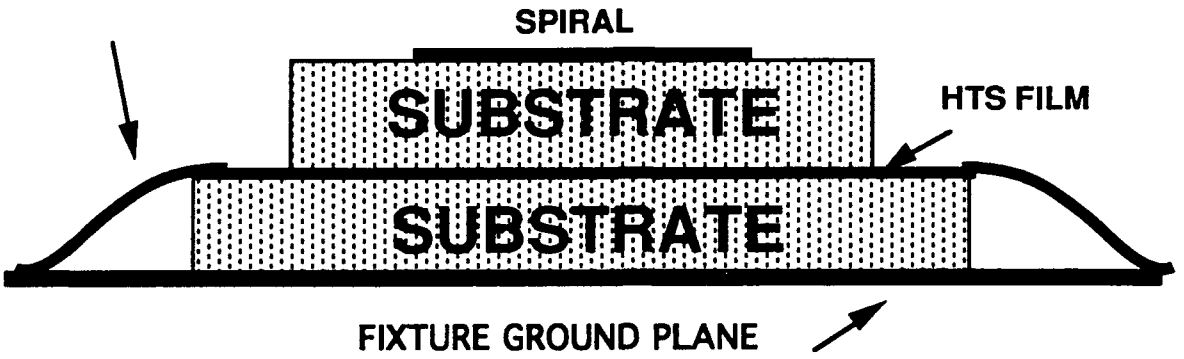

Fig. 2. Spiral resonator on microstrip with HTS ground plane.

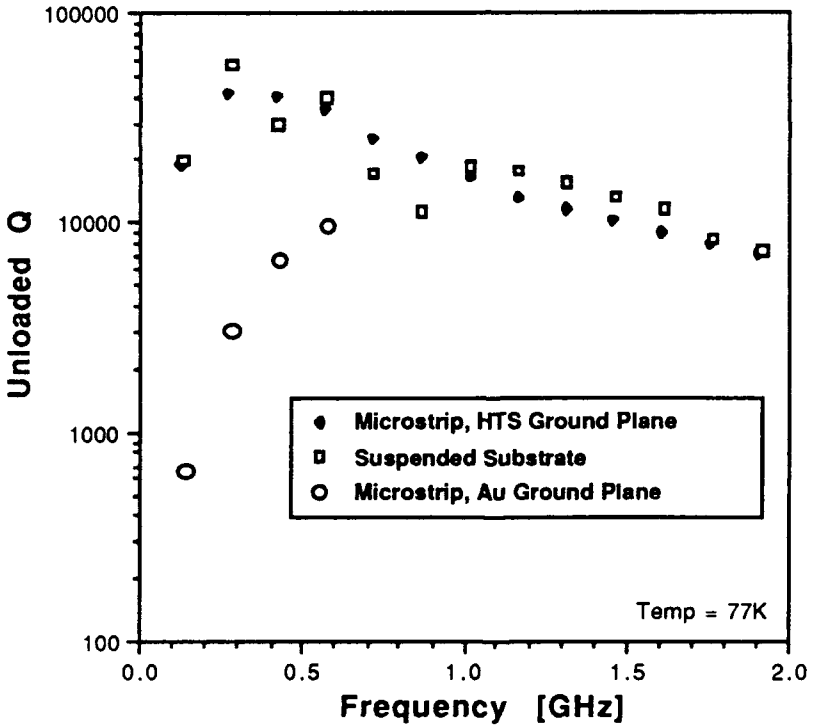

Fig. 3. Measured Q of Sample Spiral Resonator in Three Different Configurations.

III. MODELLING OF THE HTS/SUBSTRATE STRUCTURE

Because a variety of buffer layers are needed to successfully deposit a YBCO film to a substrate, we decided to investigate their effect on the performance of superconducting line circuits. Typical buffer layers have high dielectric constants and moderate to high losses. Thus their presence may cause performance degradation of the superconducting line circuits. We have used a multilayer computer program for the evaluation of the conductor and dielectric losses. The available commercial program (PCAAMT) requires the complex dielectric constant, the thicknesses of each dielectric layer, and the conductivity of the different metallization surfaces including the ground planes for the analysis of multilayer structures. Calculations can be carried out for a given frequency and a specific structure to determine the line's dielectric and conductor losses and its characteristic impedance.

We started first by investigating the effect of the dielectric constant of a single buffer layer of thickness 10^{-5} cm at 10 GHz on dielectric losses. The details of the structure are shown in Fig. 4. Fig. 5 shows the dielectric losses for a family of very high dielectric constant materials (ε_r= 100 to 500) as a function of buffer-layer-loss-tangent for a transmission line of width 0.25 cm. The calculated copper loss for these lines is 4.5×10^{-2} dB/cm, which is the dominant loss factor. However, for superconducting applications with one to two orders of magnitude improvement in surface resistance values the dielectric loss will be comparable or greater than the conductor losses. It was also recognized that buffer layers with loss tangents up to 0.001 slightly increased the dielectric losses; however, significant deterioration was seen for buffer layers with higher loss tangent and dielectric constant values. For example, for a buffer layer with a dielectric constant of 500 and loss tangent of 0.1, the dielectric loss has increased by more than an order of magnitude as shown in Fig. 5. Therefore, it is recommended to

use buffer layers with moderate dielectric constants and loss tangent values below 10^{-2} to insure high performance. As shown in Fig. 6 wider lines do not show as much deterioration with increasing loss tangent.

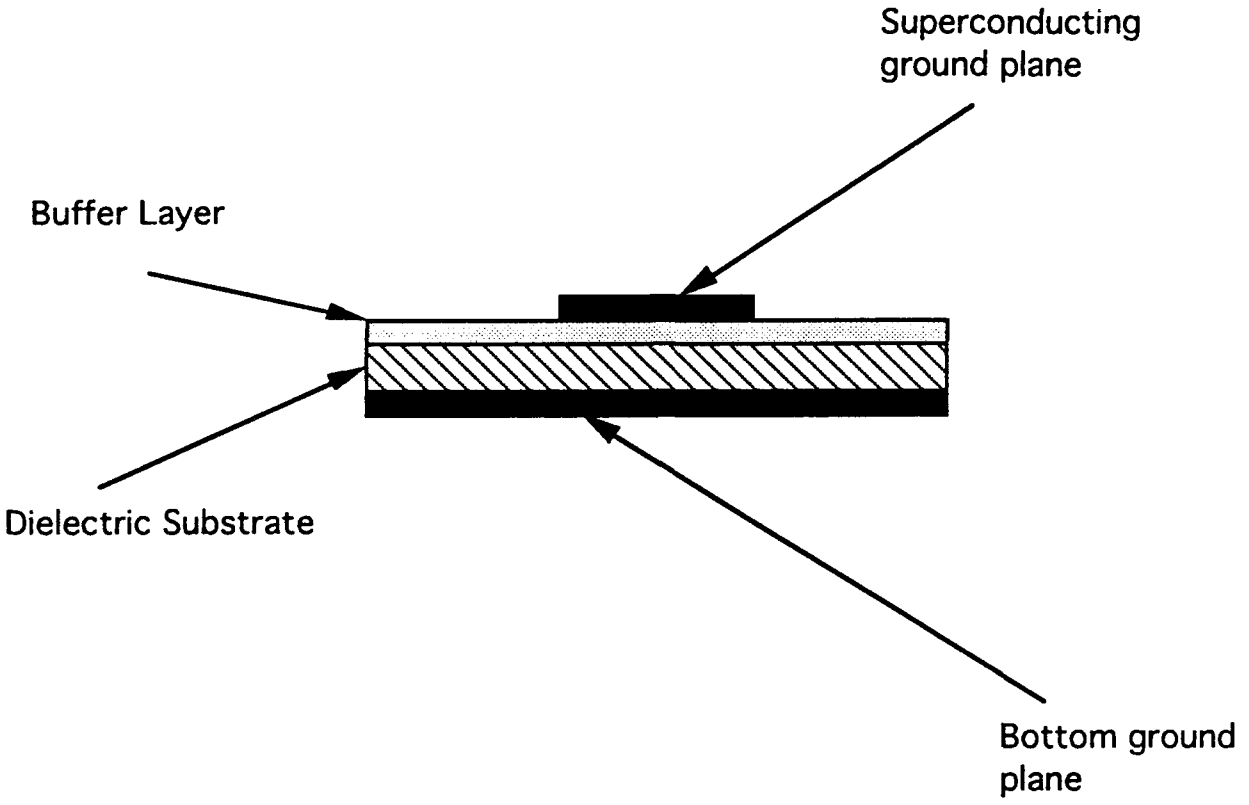

Fig. 4. Sketch of a single buffer layer microstrip line.

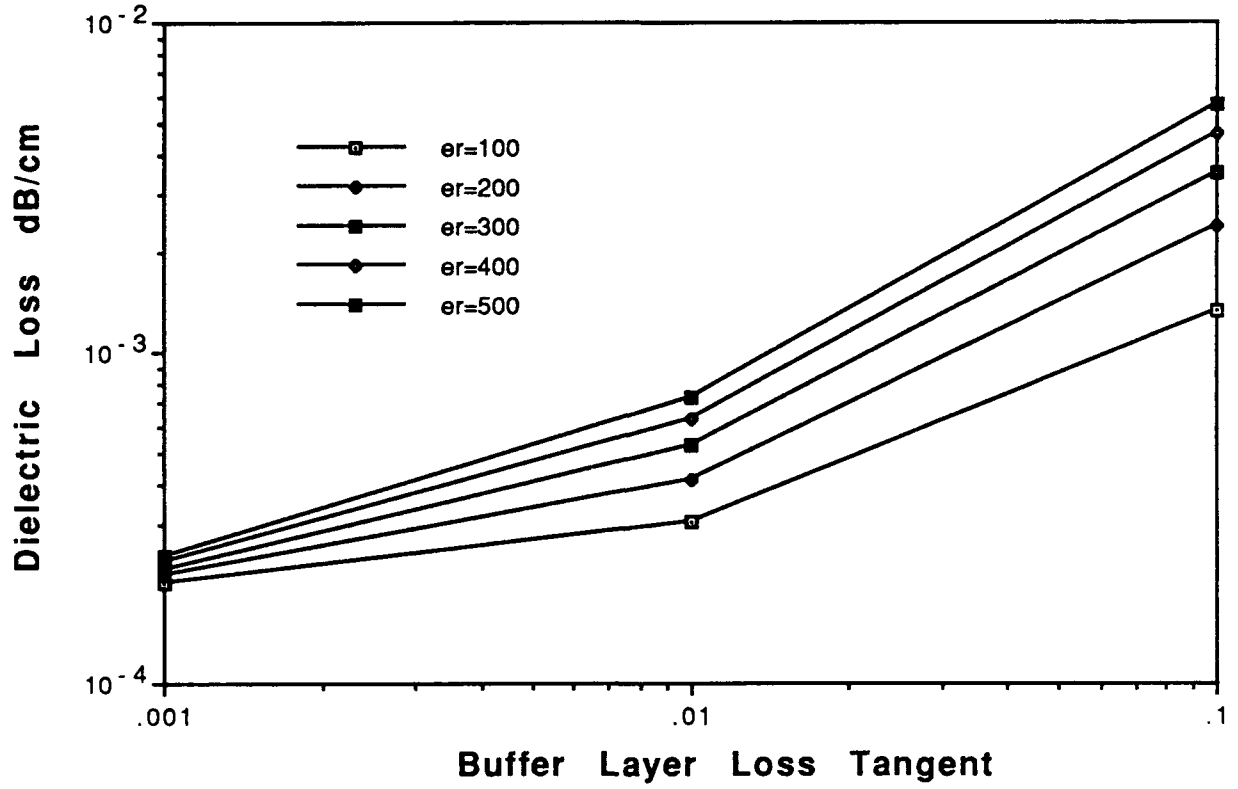

Fig. 5. Effect of single buffer layer loss tangent on a microstrip line overall dielectric loss shown for a family of different buffer layer dielectric constants ranging from ε_r= 100 to ε_r=500. The line width is w=0.25 cm, dielectric thickness h=0.0254 cm, cover height is hu=0.254cm, and buffer layer thickness= 1000 angstroms. Copper conductor loss is 0.045 dB/cm.

For a practical application Neocera suggested a two buffer layer structure for the superconducting material deposition on a low ε_r Fluoride substrate (ε_r = 5). The first buffer layer is MgO with ε_r = 9.5 (at 77K), and the second layer is YSZ with ε_r = 40 (at 77K). Neocera routinely deposits films of such buffer layers approximately 1000Å thick. Based on these values we determined the dielectric loss as a function of strip width; the calculations were carried out at three different frequencies 0.1, 1, and 10 GHz with substrate heights of 40, 25, and 10

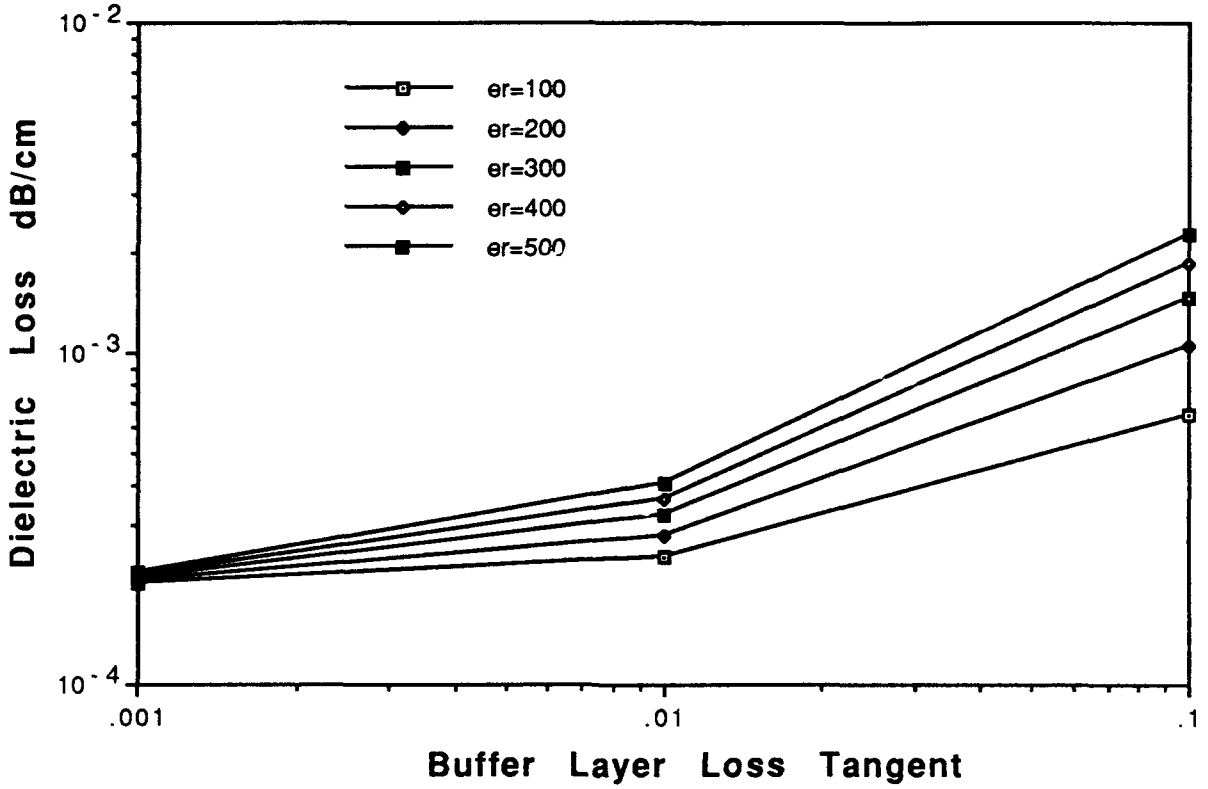

Fig. 6. Effect of single buffer layer loss tangent on a microstrip overall dielectric loss shown for a family of different buffer layer dielectric constants ranging from ε_r= 100 to ε_r=500. The line width w=0.5 cm, dielectric thickness h=0.0254 cm, cover height is hu=0.254cm, and buffer layer thickness = 1000Å. Copper conductor loss is 0.0484 dB/cm.

mils as indicated in Figs. 7, 8, and 9. At low frequencies, the effect of buffer layers was extremely slight even for narrow lines as seen in Fig. 7. However, the effect was significant for narrow lines, thinner substrates, and higher frequencies. At 10 GHz, for example, the dielectric losses of 0.05 cm wide lines are roughly twice as high as those of 0.5 cm wide lines. These dielectric loss values are still better than the copper conductor losses, but for superconductor lines with one to two

orders of magnitude improvement in conductor loss the dielectric losses will be comparable to the conductor losses.

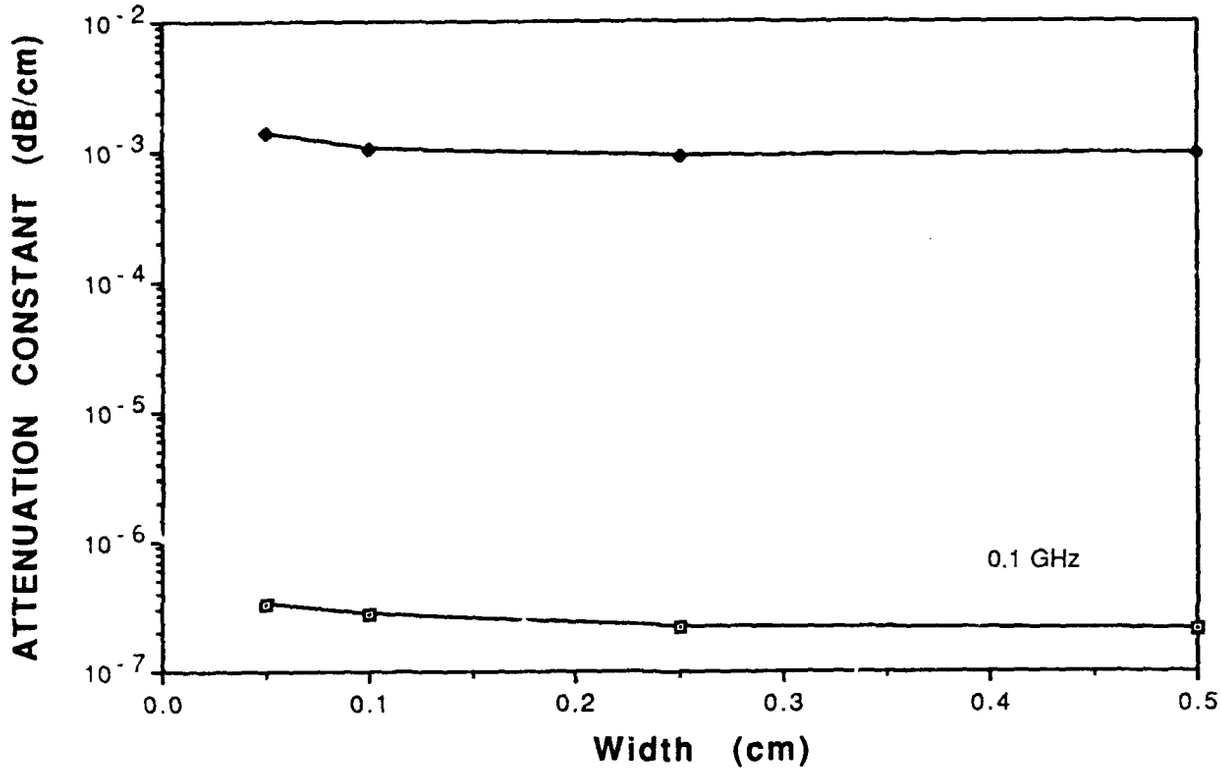

Fig. 7. Effect of buffer layer on losses; the substrate ε_r=5, thickness= 40 mils, f= 0.1 GHz, tan $\delta = 10^{-6}$, and the buffer layers are YSZ (ε_r=40, tan δ= $74.2X10^{-5}$), and MgO (ε_r=9.5, tan δ=$.62X10^{-5}$), and each having 1000Å thickness.

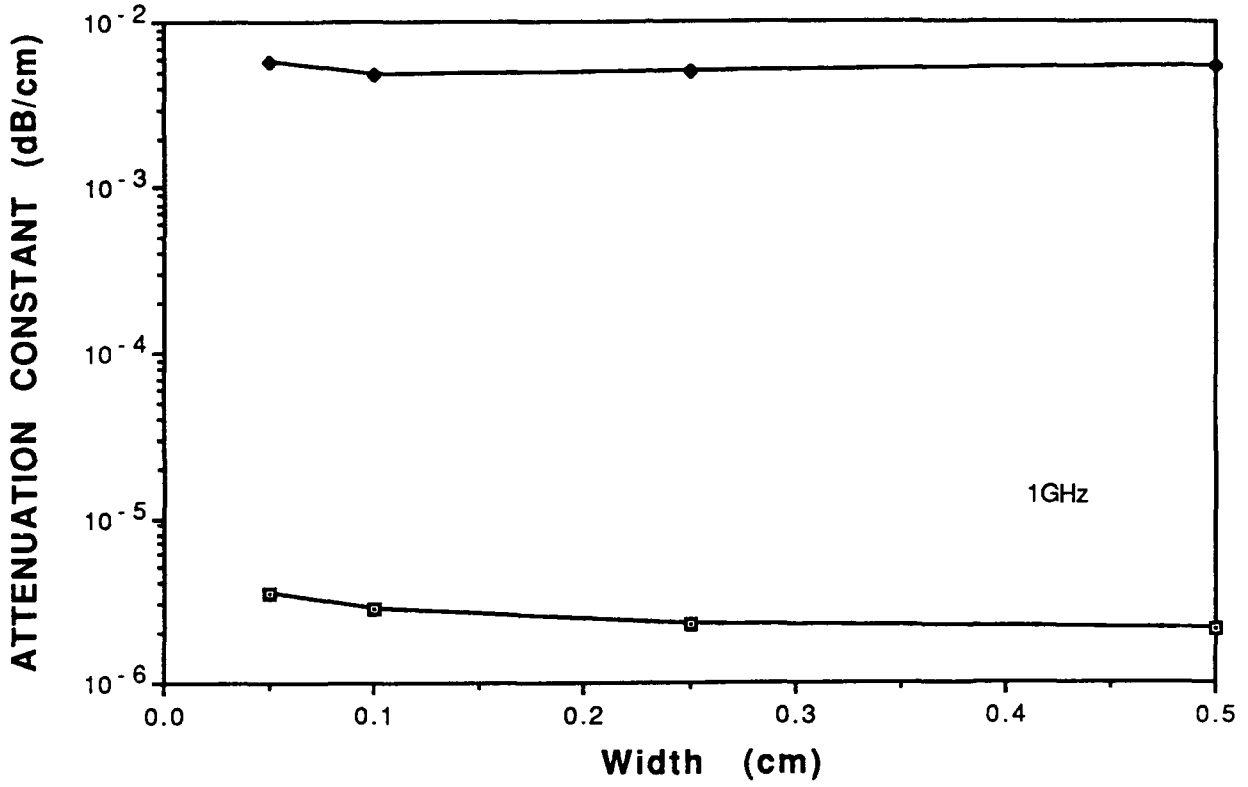

Fig. 8. Effect of buffer layer on losses; the substrate ε_r=5, thickness= 25 mils, f= 1.0 GHz, tan $\delta = 10^{-6}$, and the buffer layers are YSZ (ε_r=40, tan δ= 74.2X10^{-5}), and MgO (ε_r=9.5, tan δ=.62X10^{-5}), and each having 1000Å thickness.

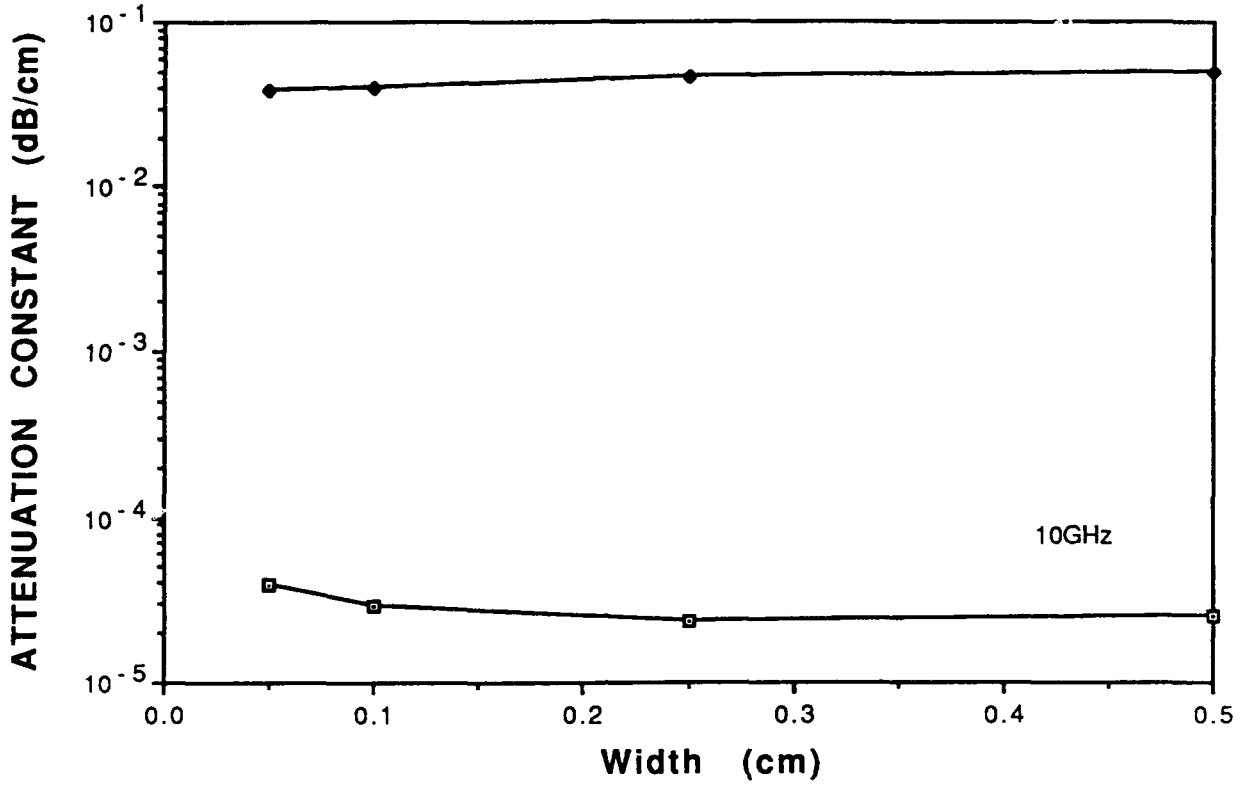

Fig. 9. Effect of buffer layer on losses; the substrate ε_r=5, thickness= 10 mils, f= 10 GHz, tan δ =10^{-6}, and the buffer layers are YSZ (ε_r=40, tan δ= 74.2X10^{-5}), and MgO (ε_r=9.5, tan δ=.62X10^{-5}), and each having 1000Å thickness.

IV. EXTENSION OF POWER HANDLING CAPABILITY FOR HTS COMPONENTS

As high temperature superconductors are being applied to an increasing number of microwave and millimeter wave components, it becomes apparent that the rf power handling capability of the current materials poses a serious limitation. Especially, for high-Q components such as resonators and filters where the magnitudes of the circulating currents are many times those of the corresponding transmission power level the tolerable signal level is in the

milliwatt range and below. Systems that require low intermodulation distortion products and a large dynamic range are particularly sensitive in this respect.

The sometimes claimed high power handling capability of certain components [1,2] often refers to the circulating power of a resonator that is still superconducting at this power level. For most communications systems this meaningless non-linear distortion sets in at much lower power levels and the system's spurious response requirement is the determining factor for the tolerable single level. In this respect, 3rd-order intercept measurements as used for active devices can be used to determine the real power handling capability of a particular superconducting component.

To improve the marginal or unsatisfactory power handling capability of a superconducting component one can rely on further improvements in the granularity and T_c on the HTS material which can be expected to occur as the state of the art progresses. It is also possible, however, by proper choice of the circuit configuration to achieve an increase in the power handling capability. A major goal of this program is to develop YBCO coatings on substrates of low dielectric constant which is vital for millimeter wave applications and is also important for improved power handling. The lower-ε substrate leads to circuits with lower current density and thus higher signal level tolerance. Furthermore, the circuit configuration itself can greatly affect the maximum current density.

As an example, narrow coupled-lines in a high-Q filter have orders of magnitude higher current densities than comparative disk resonators. Current crowding on narrow lines greatly contributes to the localized increase in current density. Proper choice of the resonator mode that avoids high current densities at the edge of the superconductor can lead to substantial improvements in power handling capability. The penalty one pays in such configurations is an increase in size. However, if the major benefit to be derived is lower loss from the

superconductive implementation, the increase in size may be a worthwhile trade-off in the overall systems requirements.

A. Mode-Type Effects

Power handling capability depends significantly on the specific propagating mode type. Take a parallel plate line structure as an example; for a given maximum electric field component 'E_0', the structure sustaining a TEM mode can handle a higher power level than one with either a TE or a TM mode. Qualitatively, the power per unit width carried by a TEM line is given by:

$$P_{TEM}=E_O^2/2Z_Oh$$

where Z_0 is a constant and given by

$$Z_o=\sqrt{\frac{\mu}{\varepsilon_o\varepsilon_r}}$$

However, the expressions for power per unit width for the TE and the TM modes are given by:

$$P_{TEM}=E_O^2q/4Z_Oh$$

$$P_{TEM}=E_O^2/4q_Oh$$

where q is less than 1 and is given by:

$$q=\sqrt{1-(f/f_c)^2}$$; f_c is the cutoff frequency

The above expressions indicate lower power handling for TE and TM modes than for TEM mode structures; and, in addition, a TM mode structure can handle more power than one supporting a TE mode.

B. Structure Type Effects

The power dissipated or stored in a two entry resonant structure is related to the power available from the source through the coupling coefficient β. At resonance, the transmission coefficient is given by

$$T(\omega)=\frac{4\beta^2}{(2\beta+1)^2}$$

while the power dissipated P_D can be related to the source power P_s by:

$$P_D=\frac{P_s}{(2\beta+1)}$$

The field distribution can be calculated as a function of the dissipated power in the resonant structure. The loaded Q_l can also be related to the unloaded Q_o by the following relation:

$$Q_o=Q_l(1+2\beta)$$

Disc vs. Rectangular Resonator:

The conductor's Q (Qc) for both the the disc and the rectangular resonator is the same and can be calculated using the following expression:

$$Q_c=h\sqrt{\mu_o\pi f_o\sigma_c}$$

where h is the thickness of the disc resonator, f_o is the disc resonant frequency, and σ_c is the conductor's conductivity. The power dissipated P_c in either structure is also given by the following relation:

$$P_c=2\sqrt{\frac{\pi f_o}{\mu\sigma}}\frac{\varepsilon_s}{h}$$

where ε_s is the stored energy. The energy stored for both the rectangular and the circular structures are given by:

$\varepsilon_s=\frac{\varepsilon_{eff}\varepsilon_o V_o^2(ab)}{4h}$ for a rectangular element with a, b dimensions.

$\varepsilon_s=\frac{\varepsilon_r\varepsilon_o V_o^2(\pi a^2)}{4h}$ for a circular disc with radius a.

The stored energy is proportional to the area of the resonator and inversely proportional to the height of the substrate. If the two structures are dissipating

the same amount of power, and even if they have the same area, the electric fields of the rectangular resonator will be higher due to the lower effective dielectric constant ε_{eff}. For a given resonant frequency, the area of the circular resonator is generally bigger than the area of the rectangular resonator. The latter is typically a straight line of narrow width b with the area given by:

$$\text{Area} = axb = \frac{c_o \pi b}{2\sqrt{\varepsilon_{eff}}\omega}$$

where c_o is the speed of light. The area of the circular resonator is:

$$\text{Area} = \pi x a^2 = \frac{c_o^2 \pi 1.841^2}{\varepsilon_r \omega^2}$$

Therefore, higher electric field values will be sustained in the rectangular line resonator as compared to the circular disc for a given dissipated power level, and it can be easily seen that the dissipated power P_c is not a function of the substrate height h.

Maximum Current Calculations:

For a circular disc, the field components for the TM_{11} are given by:

$$E_z = E_o J_1(K\rho)\cos\varphi / J_1(Ka)$$

$$H_\rho = \frac{-j}{\omega\mu\rho} E_o J_1(K\rho)\sin\varphi / J_1(Ka)$$

$$H_\varphi = \frac{-jK}{\omega\mu} E_o J_1'(K\rho)\cos\varphi / J_1(Ka)$$

which will generate two current components associated with $J = \hat{n}xH$. The maximum current component J_{max} will be at $\rho=o$ in the ρ-direction and is related to the electric field component ($E_o = V_o/h$) by:

$$J_{max} = \frac{0.5\sqrt{\varepsilon_r}}{0.5818 x 120\pi} E_o$$

Similarly, for the rectangular resonator for the Quasi-TEM mode the field components are:

$$E_z = \frac{V_o}{h}\cos\left(\frac{\pi}{a}x\right)$$

$$H_y = \frac{jV_o}{Z_c}\sin\left(\frac{\pi}{a}x\right)$$

where Z_c is the characteristic impedance of the line. The maximum current will be in the center of the line and is given by:

$$J_{max}=\frac{E_o}{Z_c}$$

which indicates higher currents for the same electric field values E_0 for the rectangular resonator as compared to the disc resonator case, except extremely narrow lines can have lower currents if

$$\left(\frac{0.5\sqrt{\varepsilon_r}}{0.5818x120\pi}E_o\right)_{TM}>\left(\frac{E_o}{Z_c}\right)_{Quasi\text{-}TEM}$$

$$\text{i.e. } \left(\frac{0.5\sqrt{\varepsilon_r}}{0.5818}\right)_{TM}>\left(\frac{120\pi}{Z_c}\right)_{Quasi\text{-}TEM}$$

For practical lines with both high ε_r (ε_r=24), and low ε_r (ε_r=5) this condition was not satisfied for the range of w/h of (.1 < w/h < 20). Figs. 10 and 11 show the ratio between the maximum current in a linear resonator compared to a disc resonator. For narrow lines, the characteristic impedance can be very high leading to a reduction in the maximum current; however, current crowding and edge effects can lead to substantially higher currents near the edges by a factor of 10. This high edge current will cause increases in line loss and spoil their Q's.

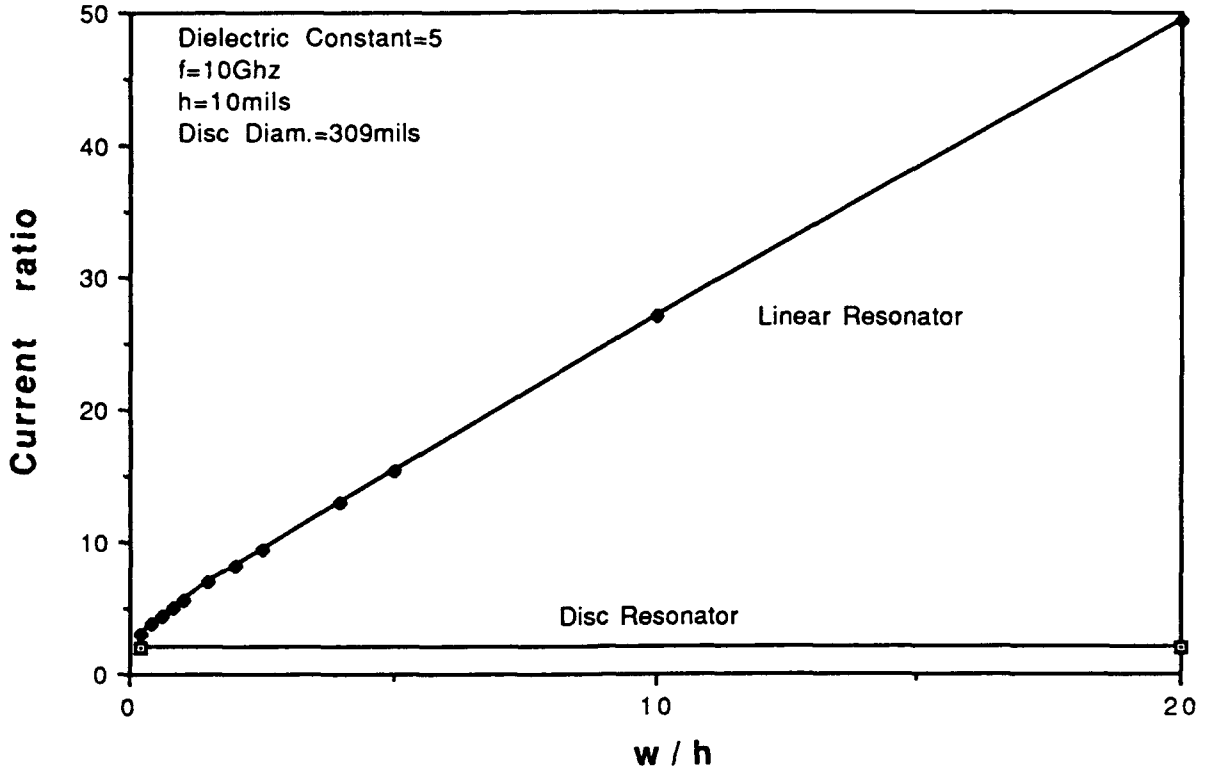

Fig. 10. Comparison between the maximum current coefficient for the disc and linear resonator as a function of the width of the line. The dielectric constant is 5, the substrate height is 10mils, and the resonant frequency is 10 GHz.

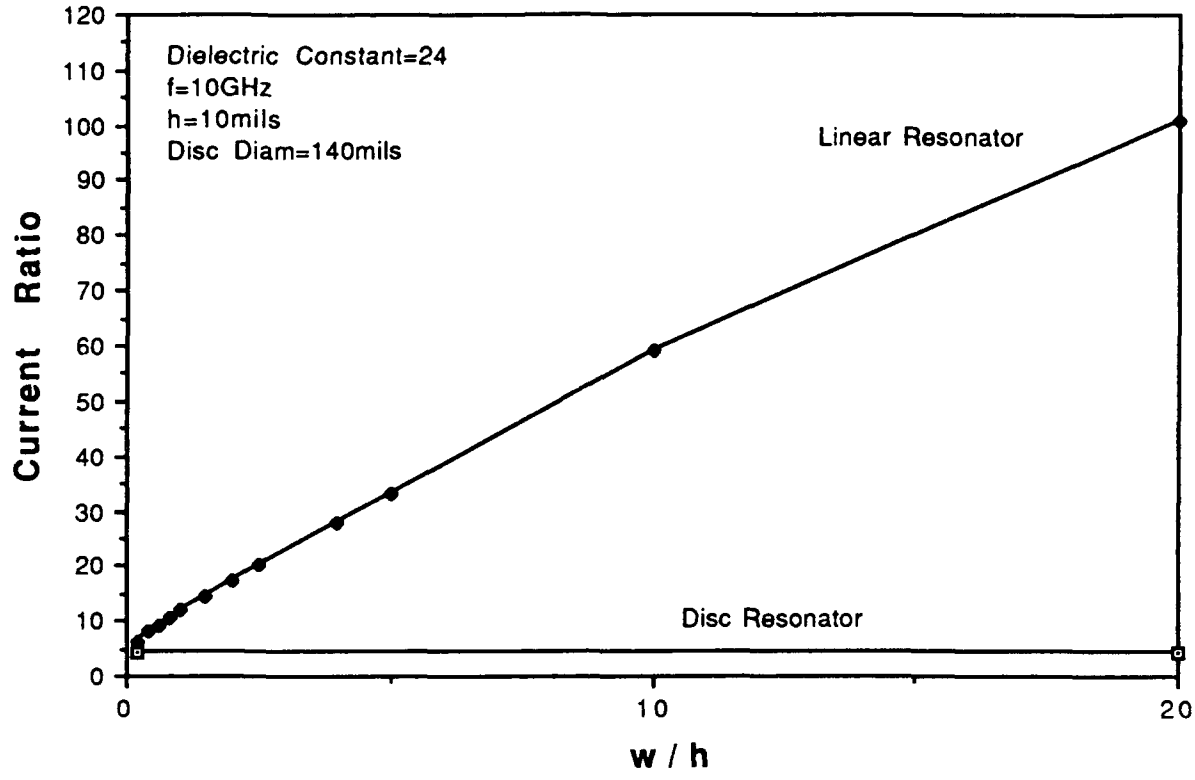

Fig. 11. Comparison between the maximum current coefficient for the disc and linear resonator as a function of the width of the line. The dielectric constant is 24, the substrate height is 10mils, and the resonant frequency is 10 GHz.

V. HTS MATERIAL DEVELOPMENT

Toward the goal of depositing high quality YBCO film on low ε, low tan δ substrates, we have undertaken two different approaches. In the first approach, we have attempted to grow YBCO films on low ε substrates such as (001) SrF_2 (ε_r = 6.19 at 77 K) and crystalline α-quart (ε_r = 4.2). In the second approach, which is mainly derived from our success in the NASA phase I program, we grow high quality YBCO films on a conventional growth substrate, followed by chemical etching of the substrate, leaving a free standing YBCO film. The YBCO film can

then be redeposited onto a custom substrate of choice. Under our NASA phase I requirements, we redeposited the films on single crystalline diamond (ε_r = 5.5). The following report summarizes our results obtained thus far.

A. YBCO on (001) SrF_2

All the initial YBCO films on (001) SrF_2 substrates were carried out without any buffer layers. These depositions were carried out mainly to understand the various possible film - substrate interfacial reactions, so that a suitable diffusion barrier (buffer layer) could be deposited. A typical ac susceptibility plot for YBCO directly on (001) SrF_2 without any buffer layer is presented in Fig. 12. The films exhibit T_c onsets around 81K with broad transition widths. The low T_c's observed are suggestive of film-substrate reactions which are currently investigated by collaborators at the Princetion University. Formation of interfacial BaF_2 compound seems to be a common occurrence in all the cases where YBCO is deposited directly on the fluoride substrates. The same results were also observed for the CaF_2 and MgF_2 cases. The results suggest the need for an appropriate buffer layer or combination of buffer layers. In order to grow a high quality YBCO, the buffer layer needs to be (100) oriented forming a structural template for the YBCO film deposition. Among the various cubic buffer layers considered, MgO seemed to be the best choice. It has a lattice parameter of 4.21Å [3] and has a lattice mismatch of only about 2.5% with respect to SrF_2, if the epitaxial relationship {110} MgO {001} SrF_2 is maintained. Further, it is also known that MgO has low energy cleavage planes and fast diffusion on these neutral planes can make epitaxial growth possible down to remarkably low temperatures (approximately 1/10 of the melting poing) [4,5]. Taking advantage of this property we have carried out a series of depositions in various temperature and pressure regimes. During these studies we observed that one of the most important

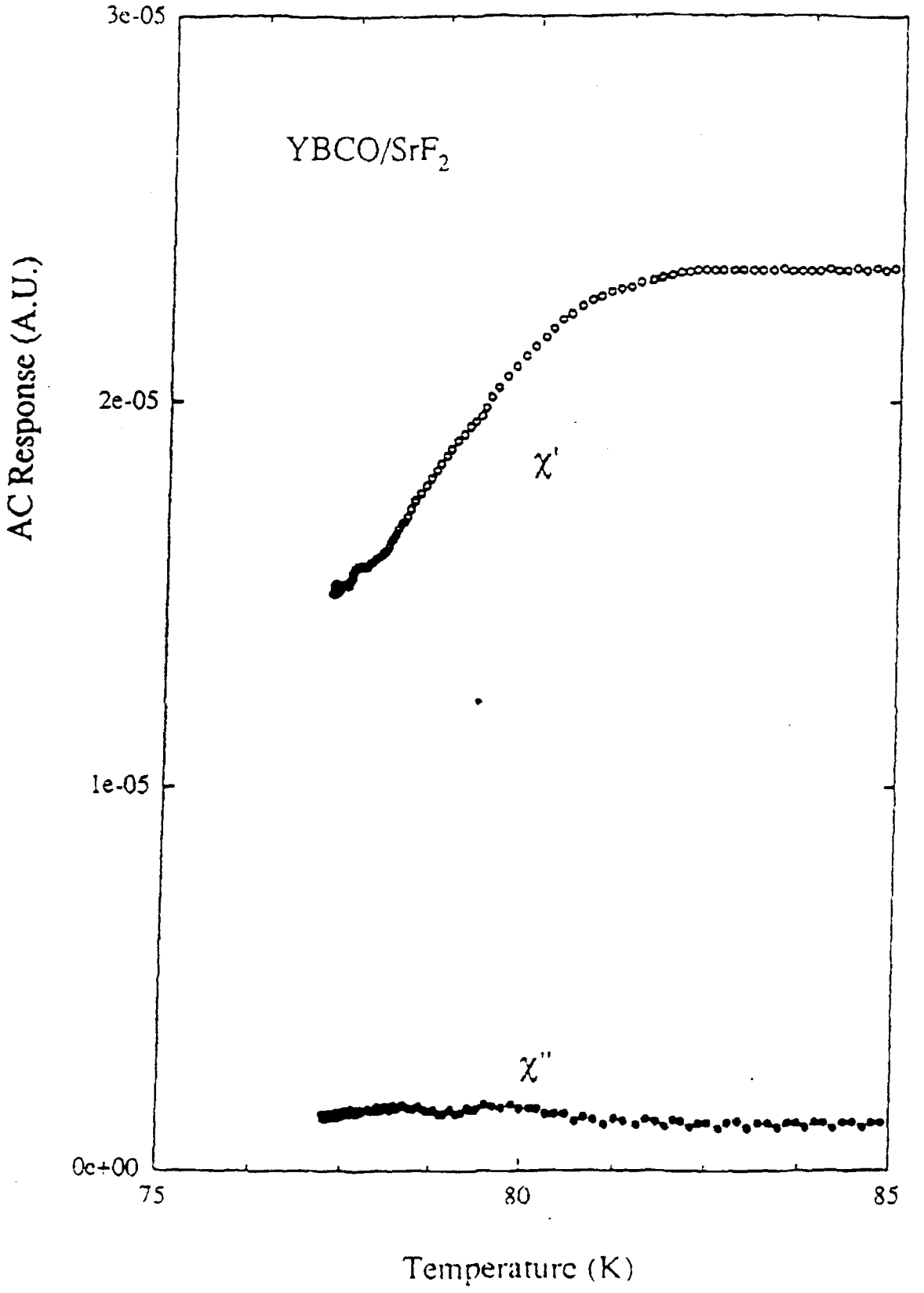

Fig. 12. AC susceptibility plot for YBCO films directly on (001) SrF_2.

parameters in growing high quality MgO films on SrF_2 substrates is the oxygen partial pressure during the growth. The x-ray data presented in Fig. 13 indicates a high degree of epitaxial growth as seen by the (100) oriented growth (2θ = 42.9°). These films are grown at temperatures ~ 500°C and oxygen partial pressures ~ 1mTorr. It may be mentioned here that most of the conventional buffer layers such as yttria stabilized zirconia (YSZ), CeO_2 etc., are grown at oxygen partial pressures two orders of magnitude higher than the pressures used for MgO growth. Further, the temperature range at which these buffers are grown (800°C) on substrates like R-plane sapphire etc., do not permit a similar growth on SrF_2 substrates due to chemical reactions at the film-substrate interface.

YBCO film deposition has been carried out on the (100) MgO buffered (001) SrF_2 and Fig. 14 shows a typical ac susceptibility data on one of the films. The films exhibit T_c onset temperatures around 83 K with transition widths of ~ 3-4 K. The lower T_c's observed in the present case relative to films deposited on $LaAlO_3$ could be due to possible diffusion of the impurity phases from the film-substrate interface, the traces of which are seen in the x-ray profiles presented in Fig. 15. The figure shows predominantly c-axis oriented YBCO growth. It may be noted that even though the MgO buffer layer on SrF_2 substrate is grown at a relatively low temperature of ~ 500° C, the subsequent YBCO film growth was carried out at temperatures ~ 700°C. At these growth temperatures, chemical reactions at the film-substrate interface and diffusion of impurities across the interface seems to be occurring, which suggests the need for a second buffer layer.

As a second buffer layer, YSZ has been deposited over (100) MgO buffered (001) SrF_2 substrates, prior to the YBCO deposition and preliminary ac susceptibility data of one of the films is shown in Fig. 16. Although T_c onset temperatures are around 82 K (as in the case of the single buffered substrates), the transition widths are reduced to < 2 K, suggesting significant improvements

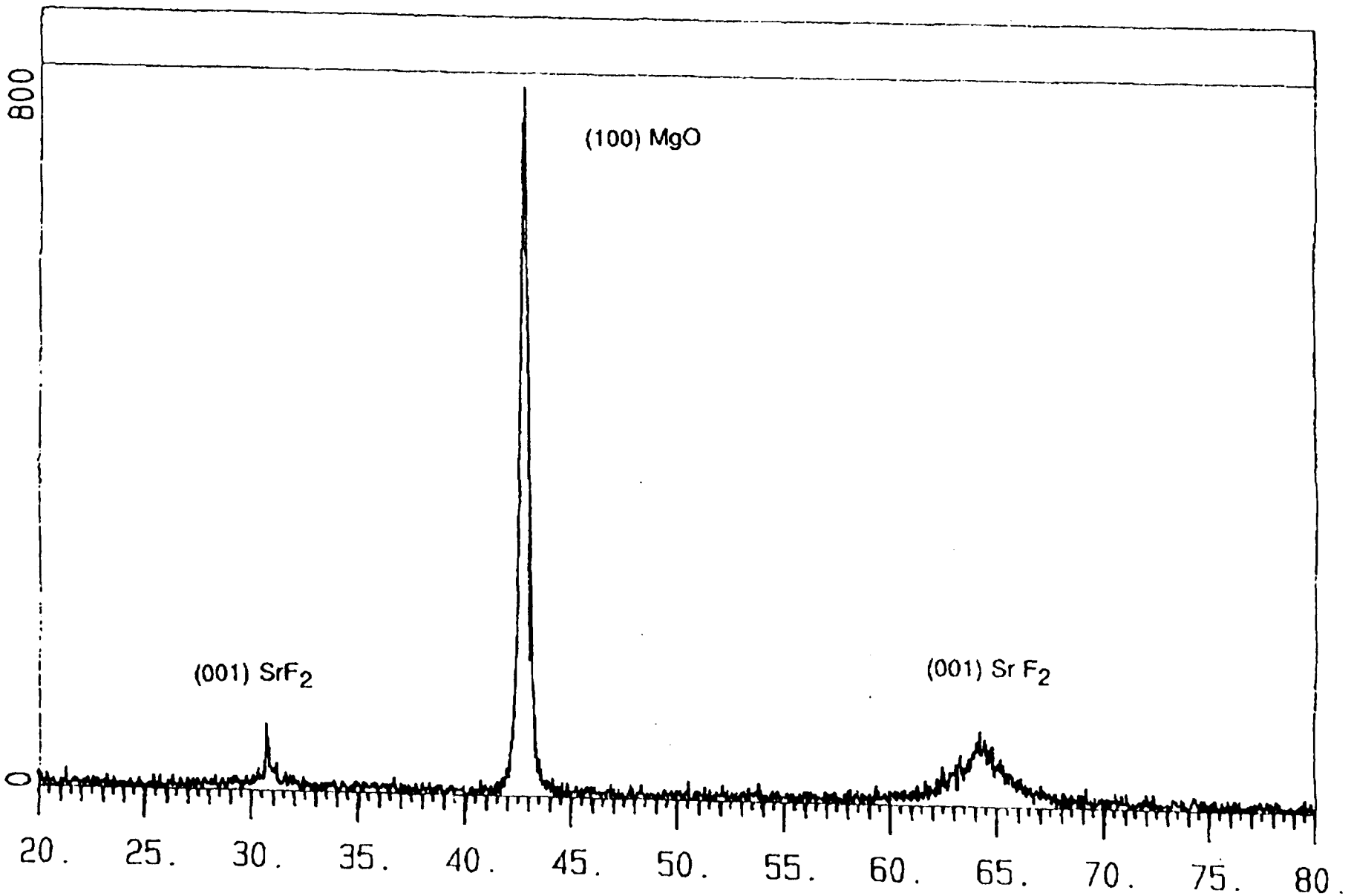

Fig. 13. X-ray diffraction data for MgO films deposited on (001) SrF_2 Substrates.

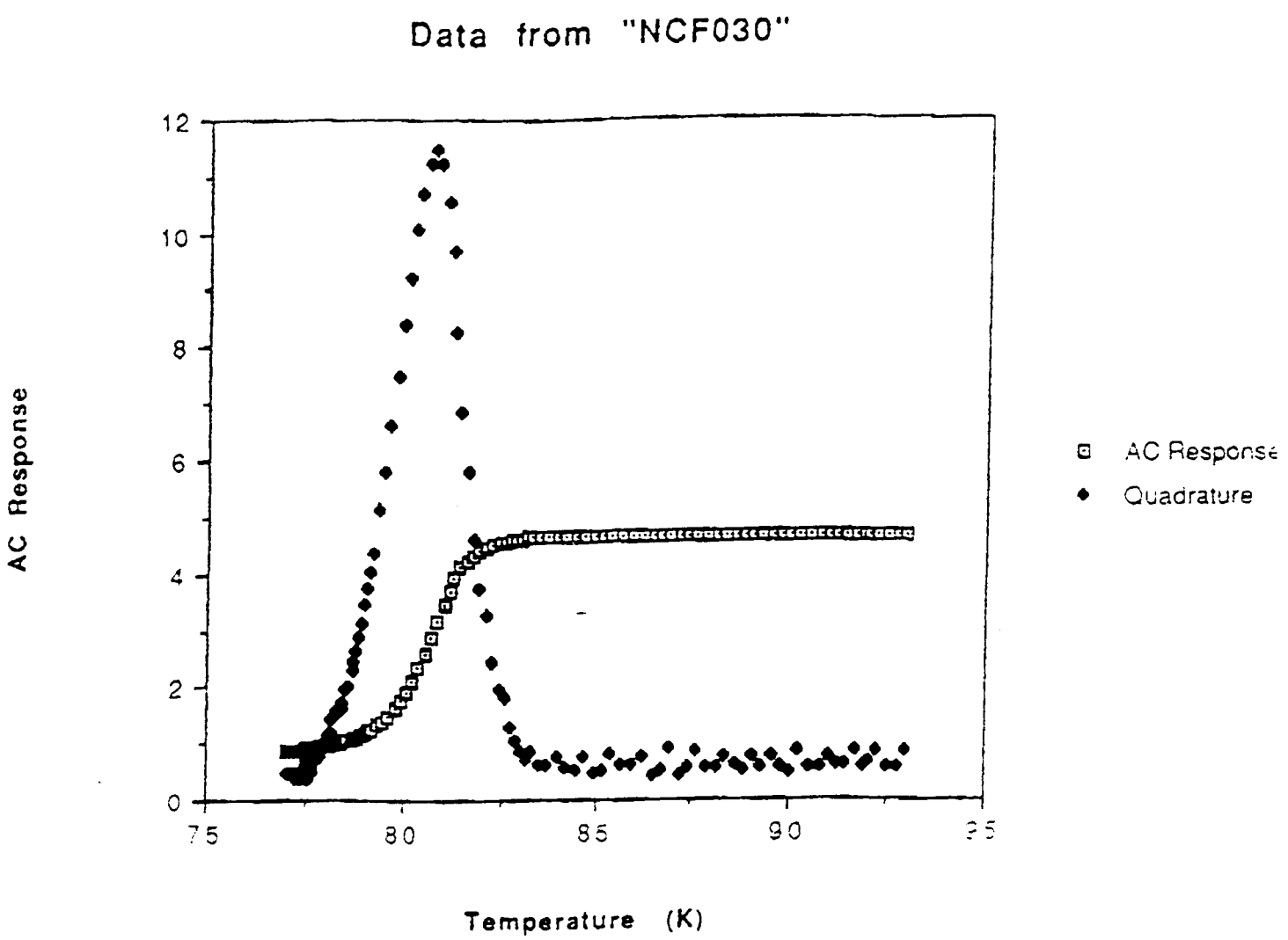

Fig. 14. AC susceptibility data for YBCO films on (100) MgO buffered (001) SrF_2.

in the film quality. These results also suggest further improvements by optimizing the YSZ buffer layer growth. It may be mentioned here that YSZ and YBCO film depositions have been carried out, in these specific cases, around 700°C, which is considerably lower than the temperatures (800°C) at which high quality films are grown on substrates such as $LaAlO_3$ and R-plane sapphire. It is generally observed that YBCO films deposited at temperatures ~ 700°C (as in the present case) are rather poor in quality, often exhibiting lower transition temperatures even when deposited on conventional substrates like $LaAlO_3$. A high quality film necessitates growth at higher optimal temperatures, and the

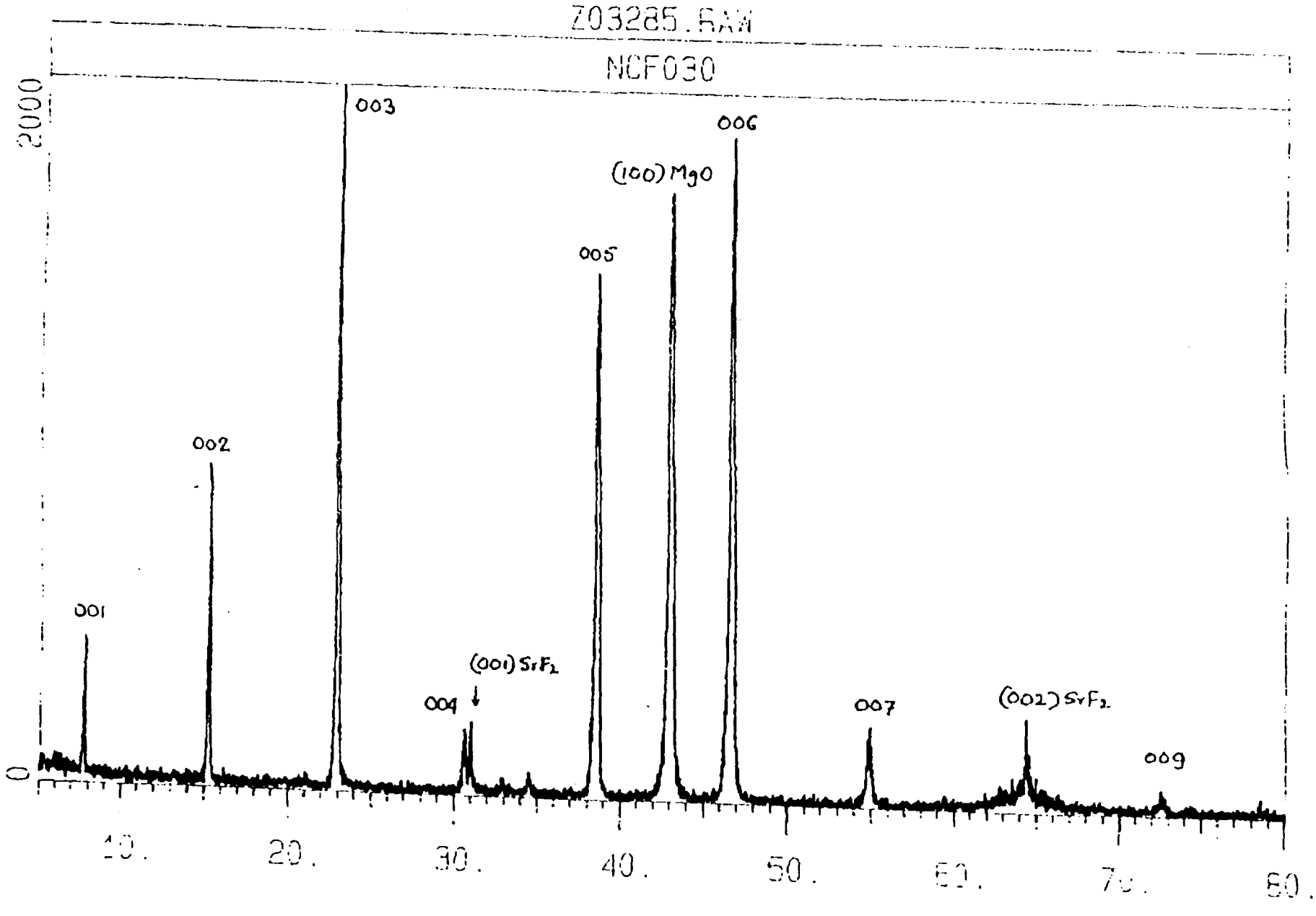

Fig. 15. X-ray diffraction data for a typical YBCO film showing highly c-axis oriented growth.

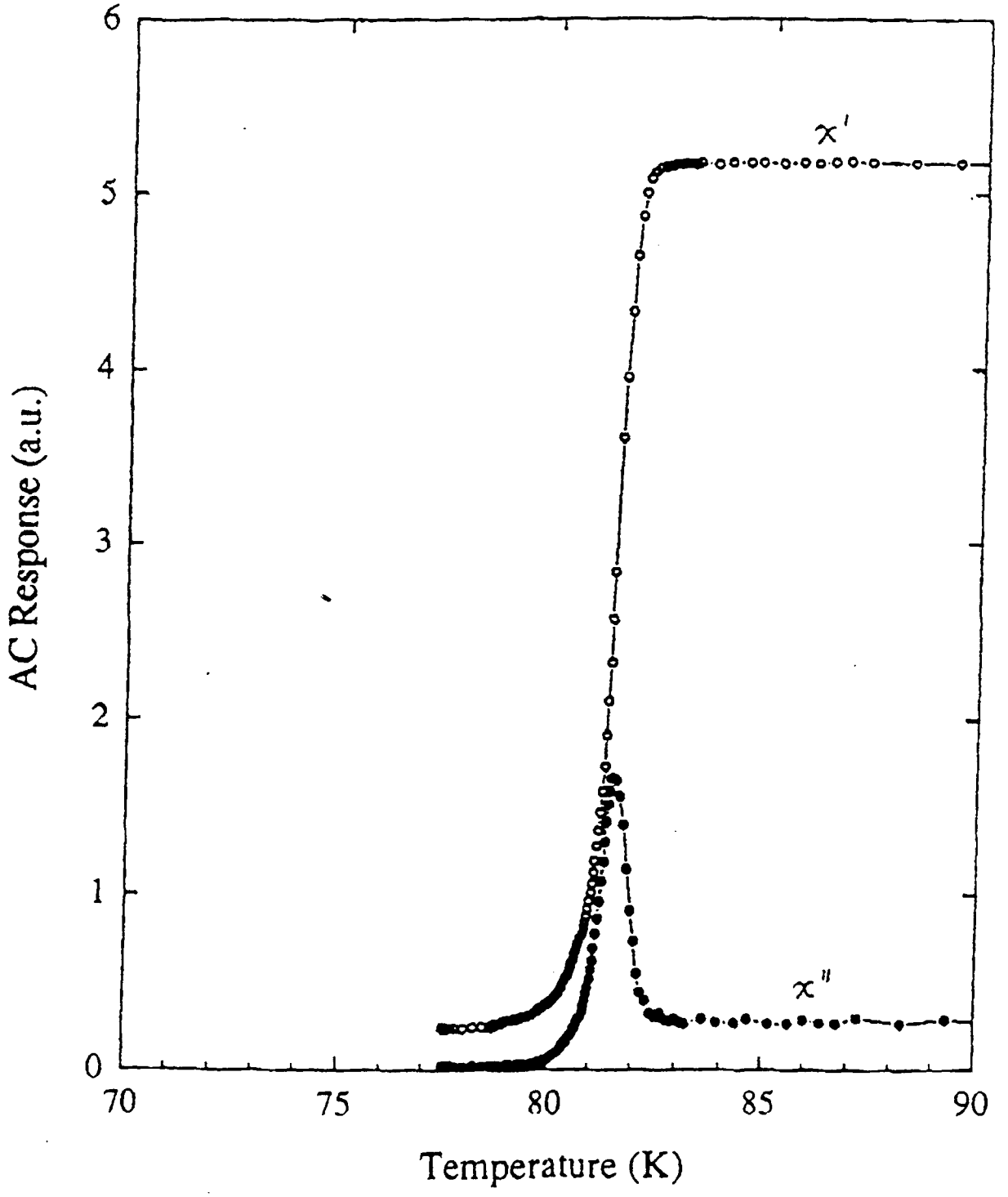

Fig. 16. AC susceptibility plot for YBCO films with YSZ/MgO buffer layers on SrF_2.

large temperature range available to us (from 700°C to 800°C) suggests a possibility of growing good quality films. As already mentioned in the report, the high chemical reactivity of the fluoride substrates at elevated temperatures offsets the advantages associated with their desirable microwave properties. The growth of the second buffer layer is being optimized at present to alleviate the contamination problem. If (100) oriented YSZ could be grown epitaxially on (100) MgO buffered SrF_2 substrates, this would also indicate the possibility of growing high quality YBCO films. At present, the primary objective is to grow YSZ as a second buffer layer and we are evaluating the structural characteristics of YSZ buffer by using x-ray diffraction and optimizing the deposition parameters.

B. YBCO on Quartz

We have been exploring the possibility of Y-cut quartz (ε_r = 4.2) as a potential substrate material. Our experiments show promising results as seen by Fig. 17. The figure shows ac susceptibility data for a typical YBCO film on Y-cut quartz substrate with a 1000 Å thick YSZ buffer layer. The films exhibit T_c onsets around 85 K with ~ 5K transition width. We are continuing with these experiments. One of the major problems with the quartz substrate is the phase transformation from α-β phase occurring at the temperature of ~570°C, which makes the material susceptible to thermal shock. The low thermal expansion coefficient of quartz imposes additional restrictions on its potential use as a substrate.

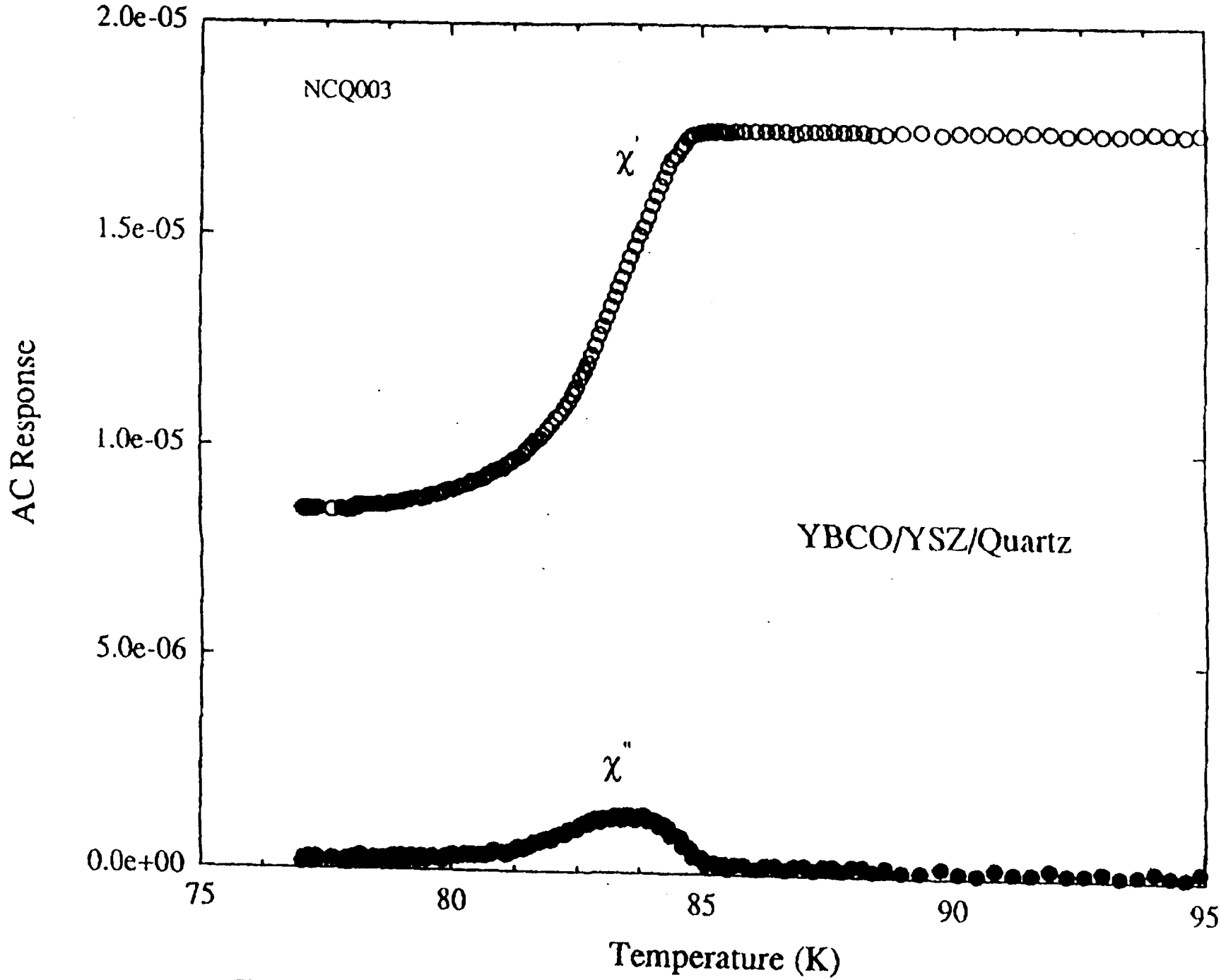

Fig. 17. AC susceptibility data for YBCO films on y-cut quartz.

C. Free Standing YBCO Films

Under a NASA phase I program, we have recently explored the feasibility of forming free standing YBCO films. In this technique, high quality films are first grown on a conventional growth substrate, followed by a selective removal of the substrate, leaving a well oriented free standing high T_c film membrane. These films can then be redeposited on any substrate of choice. In the present case, as per our phase I requirements, we have been able to successfully redeposit the films on diamond substrates (ε_r=5.5). The superconducting properties of the redeposited films on diamond have been measured and Fig. 18 shows a typical dc resistance plot of the films as a function of temperature. The films exhibit encouraging T_c onset temperature around 85 K. A further optimization of the process parameters could lead to enhanced film properties.

In the above mentioned case though we have used diamond as the substrate, this technique in principle, can be extended to any substrate. The substrates being considered for growing the YBCO film are silicon and sapphire. Silicon is the easiest to chemically etch for creating a free-standing YBCO film. However, the quality of YBCO films on sapphire with the resultant Tc and transition width has been superior to that on silicon. To create a free-standing YBCO film, sapphire could possibly be mechanically lapped and polished to a thickness close to 25 microns and then chemically etched further with a hot phosphoric acid solution (280 degrees C). The monitoring of the substrate thickness during the thinning process can be accomplished by optical means. However, the mounting of the substrate during the use of the hot etchant presents a real problem. We have used our multilayer substrate computer program discussed in Section III to determine the electrical effect of epoxying the 25 micron sapphire layer with the YBCO film onto a much thicker, low dielectric constant (e.g. 4.5) substrate such as quartz or cordierite. For the case of a 10 mil

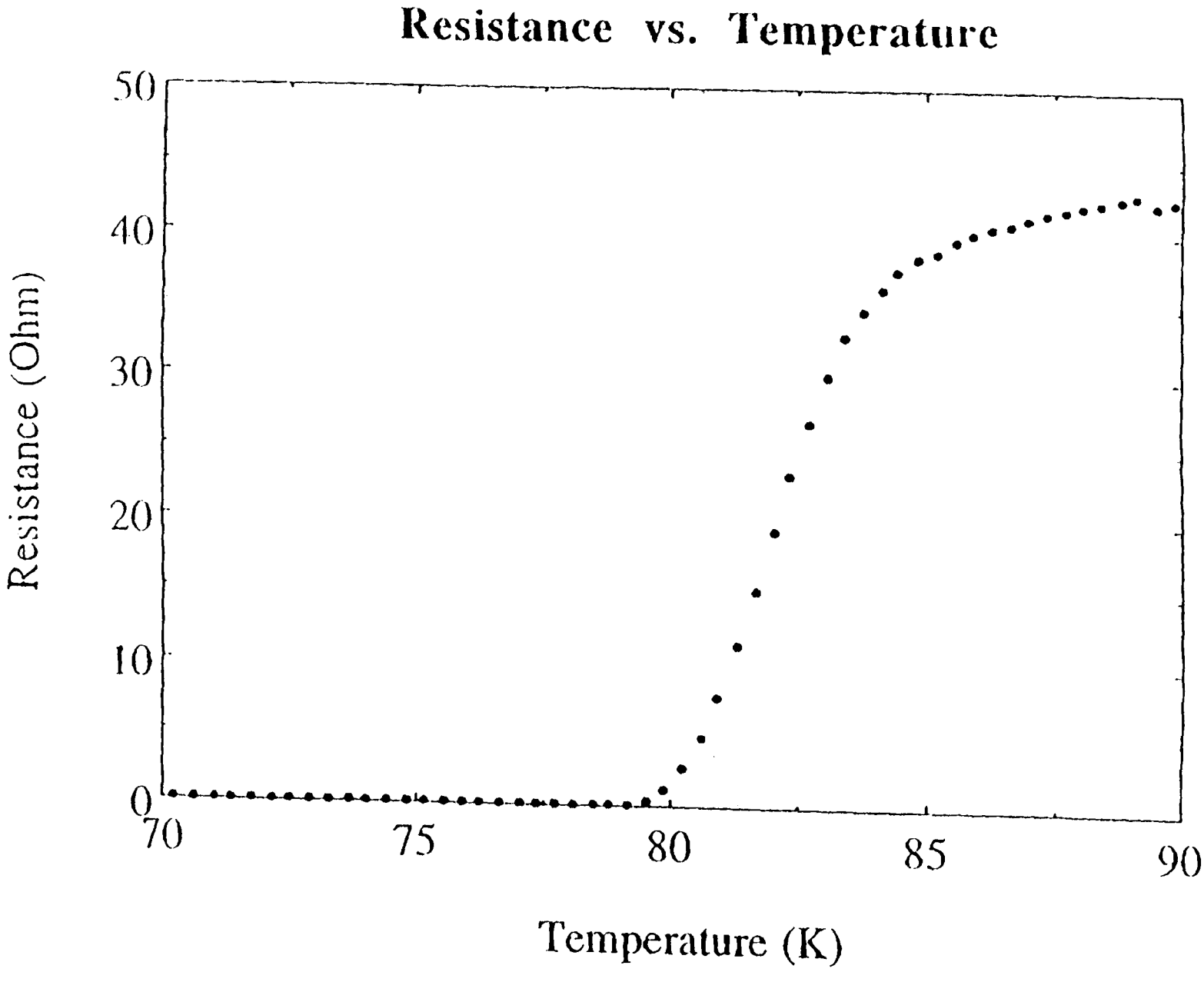

Fig. 18. DC resistance of redeposited YBOC films on diamond as a function of temperature.

thick quartz or cordierite, the presence of the sapphire layer would only change the wavelength of a microstrip line by 7 % and the characteristic impedance by 3 %, a small amount that could easily be accounted for in circuit modelling. If this process works without the need for the hot chemical etch, then the substrate mounting problem goes away because a low viscosity epoxy such as TRA-CON's material (TRA-BOND 2115) can be cured at temperatures below 65 degrees C.

References

[1]. Z. Y. Shen, et al., "High-Tc Superconductor Sapphire Microwave Resonator with Extremely High Q-Values up to 90K," Digest IEEE MTT Symp., Albuquerque, pp. 193-196, June 1992.

[2]. C. Wilker, et al., "5 GHz High-Temperature Superconductor Resonators with High Q and Low Power Dependence up to 90K", IEEE Trans. MTT, Vol. 39, pp. 1462-1467, Sept. 1991.

[3]. American Society for Testing Materials, Power diffraction files, card no. 4-829.

[4]. S. Yadavali et al. Phys. Rev. B 1, 7961 (1991).

[5]. L. D. Chang et al., Appl. Phys. Lett 60, 1753 (1992).